



**HAL**  
open science

## Reactivity of performic acid with organic and inorganic compounds: from oxidation kinetic to reaction pathways

Christelle Nabintu Kajoka, Johnny Gasperi, S. Brosillon, Emilie Caupos, Emmanuelle Mebold, Marcos Oliveira, Vincent Rocher, Ghassan Chebbo, Julien Le Roux

### ► To cite this version:

Christelle Nabintu Kajoka, Johnny Gasperi, S. Brosillon, Emilie Caupos, Emmanuelle Mebold, et al.. Reactivity of performic acid with organic and inorganic compounds: from oxidation kinetic to reaction pathways. *ACS ES&T Water*, 2023, 3 (9), pp.3121-3131. 10.1021/acsestwater.3c00279 . hal-04195028

HAL Id: hal-04195028

<https://enpc.hal.science/hal-04195028v1>

Submitted on 4 Sep 2023

**HAL** is a multi-disciplinary open access archive for the deposit and dissemination of scientific research documents, whether they are published or not. The documents may come from teaching and research institutions in France or abroad, or from public or private research centers.

L'archive ouverte pluridisciplinaire **HAL**, est destinée au dépôt et à la diffusion de documents scientifiques de niveau recherche, publiés ou non, émanant des établissements d'enseignement et de recherche français ou étrangers, des laboratoires publics ou privés.



Distributed under a Creative Commons Attribution - NonCommercial 4.0 International License

1    Reactivity of performic acid with organic and  
2    inorganic compounds: from oxidation kinetic to  
3    reaction pathways

4    *Christelle Nabintu Kajoka*<sup>1</sup>, *Johnny Gasperi*<sup>2</sup>, *Stephan Brosillon*<sup>3</sup>, *Emilie Caupos*<sup>1</sup>,  
5    *Emmanuelle Mebold*<sup>5</sup>, *Marcos Oliveira*<sup>4</sup>, *Vincent Rocher*<sup>4</sup>, *Ghassan Chebbo*<sup>1</sup>, *Julien Le*  
6    *Roux*<sup>1,\*</sup>

7    1 LEESU, Ecole des Ponts, Univ Paris Est Creteil, F-94010 Creteil, France

8    2 LEE - Laboratoire Eau et Environnement, Université Gustave Eiffel, F-44344 Bouguenais,  
9    France

10   3 IEM - Institut Européen des Membranes, Université de Montpellier, F-34090 Montpellier,  
11   France

12   4 SIAAP - Service Public de l'assainissement Francilien (SIAAP), Direction Innovation, F-  
13   92700 Colombes, France

14   5 Observatoire des Sciences de l'Univers OSU-EFLUVE, plateforme PRAMMICS,  
15   Université Paris Est Créteil, CNRS, F-94010, Créteil, France

16   \*Corresponding author: Tel.: +33(0)182392080; e-mail: [julien.le-roux@u-pec.fr](mailto:julien.le-roux@u-pec.fr)

17

18 KEYWORDS

19 organic peracid, micropollutants, kinetic rate constants, wastewater, oxidation byproducts

20 SYNOPSIS

21 This work describes the kinetics of performic acid autodecomposition and oxidation of organic  
22 compounds, and the most reactive functional groups leading to oxidation byproducts.

23 ABSTRACT

24 Performic acid (PFA) has gained interest as an alternative chemical disinfectant for wastewater  
25 (WW) treatment, but its reactivity with WW constituents remains poorly understood. This study  
26 evaluated PFA's ability to oxidize 45 inorganic and organic compounds commonly found in  
27 WW (amino acids, simple organic compounds with specific functional groups, e.g., amines and  
28 phenolic compounds, and pharmaceutical micropollutants). PFA does not react with most major  
29 ions, except for iodide ion, and reacts with iron(II) in the absence of phosphate buffer. While  
30 many organic molecules do not react with PFA, compounds containing reduced-sulfur moieties  
31 (e.g., thioether or thiol) are the most reactive (i.e., ranitidine, benzenethiol and 3-  
32 mercaptophenol), followed by compounds with tertiary amine groups (e.g., lidocaine). The  
33 reactions follow second-order kinetics with respect to both organic compounds and PFA  
34 concentrations. Similar trends were observed in real WW effluents, although removals of  
35 pharmaceuticals were lower than expected due to the probable consumption of PFA by WW  
36 constituents (dissolved organic carbon, other micropollutants, or transition metals). The results  
37 highlight PFA's selective reactivity with specific functional groups, and a low transformation  
38 of compounds mostly through oxygen addition (e.g., S-oxide or sulfonyl compounds formed  
39 from thiol and thioether moieties and N-oxides from amine groups) with similar mechanisms  
40 to peracetic acid.

## 41 1. INTRODUCTION

42 Among organic peracids, performic and peracetic acids (PFA and PAA, respectively) have  
43 recently emerged in wastewater (WW) treatment as alternative disinfectants because of their  
44 efficiency against a wide range of microorganisms<sup>1-3</sup> and because they are easy to implement  
45 technically.<sup>4</sup> The effectiveness of PFA has been demonstrated for disinfecting primary,<sup>2</sup>  
46 secondary,<sup>5,6</sup> and tertiary<sup>7</sup> WW, as well as combined sewer overflow (CSO) reservoirs,<sup>8,9</sup> with  
47 faster disinfection kinetics than PAA and/or chlorine.<sup>5,10</sup> Furthermore, peracids form very few  
48 disinfection byproducts (DBPs) compared to traditional disinfectants such as chlorine or  
49 ozone.<sup>3,7,11</sup> Under typical water treatment conditions (oxidant < 10 mg/L), the formation of  
50 halogenated DBPs and N-nitrosamines by PFA and/or PAA is negligible.<sup>6,12</sup> In addition, the  
51 use of PFA has been associated with the absence of toxicological effects in disinfected  
52 secondary WW.<sup>13,14</sup>

53 Due to its instability, PFA is not commercially available as a ready-to-use chemical solution  
54 and must be produced on-site through the reaction ((1) between hydrogen peroxide (H<sub>2</sub>O<sub>2</sub>) and  
55 formic acid (FA), which can be acid-catalyzed by a strong acid, typically sulfuric acid.<sup>15</sup> As the  
56 reaction is reversible, the resulting solution is a quaternary equilibrium mixture always  
57 containing FA, water, and two oxidants, PFA and H<sub>2</sub>O<sub>2</sub>. At the industrial scale, Kemira Oyj has  
58 developed a PFA production system that has already been implemented in Italy, Germany, and  
59 France.<sup>5,16</sup>



61 In addition to its disinfectant properties, the oxidation potential of PFA (1.537 V/Standard  
62 Hydrogen Electrode, SHE) is higher than those of H<sub>2</sub>O<sub>2</sub> (1.349 V/SHE), PAA (1.361 V/SHE),  
63 and chlorine (1.288 V/SHE), but lower than that of ozone (1.720 V/SHE).<sup>17</sup> Despite the growing  
64 use of PFA, little attention has been paid to its ability to react with the organic and inorganic

65 compounds commonly present in WW. A poor removal (<8%) of 8 pharmaceutical  
66 micropollutants was previously reported from primary-treated WW (dissolved organic carbon  
67 = 90–110 mg/L) with a PFA dose of 6 mg/L.<sup>18</sup> Bisphenol-A was not degraded by PFA in  
68 deionized water and within 1 hour of reaction.<sup>7</sup> Ragazzo et al.<sup>5</sup> also found that PFA had poor  
69 oxidation power toward phenols (at PFA doses of 0.7–1.4 mg/L for 14–30 min) or hormones  
70 such as estrone (at doses of 2–20 mg/L for 30 min). As PAA and PFA have been identified as  
71 weak oxidants for the removal of organic micropollutants, they require activation in order to  
72 become effective oxidizers. The activation of PAA has already been tested using transition  
73 metals ( $\text{Cu}^{2+}$ ,  $\text{Co}^{2+}$ ,  $\text{Fe}^{2+}$ , and  $\text{Mn}^{2+}$ ) or UV irradiation,<sup>19,20</sup> which has been proven to enhance  
74 the degradation of organic compounds.

75 This study aimed to acquire a deeper understanding of the reactivity of PFA and its oxidation  
76 potential toward substances containing various chemical functional groups. Specifically, the  
77 study aimed to: 1) investigate the reactivity of PFA in pure solutions by examining its  
78 consumption by various organic and inorganic compounds potentially present in WW; 2)  
79 determine the kinetic rate constants of decomposition of some simple organic compounds and  
80 pharmaceutical compounds by PFA; 3) evaluate some factors that influence the reaction  
81 kinetics (e.g., WW matrix, pH); and 4) identify some transformation products and elucidate the  
82 reaction pathways. To the best of our knowledge, this is the first study to address these  
83 objectives.

## 84 2. MATERIALS AND METHODS

85

### 86 2.1. Chemical Reagents

87 All the solvents and chemicals were used as received without further purification. Details  
88 regarding chemicals (purity and suppliers) are provided in Text S1 (Supporting Information,

89 SI). The solutions of organic compounds were prepared in methanol, and working solutions  
90 were obtained by dilution in deionized (DI) water (Milli-Q, 18 MΩ·cm).

## 91 2.2. PFA Preparation and Measurement

92 PFA was prepared using a method developed by Kemira (KemConnect DEX) and adapted by  
93 Nihemaiti et al.,<sup>21</sup> consisting of two steps (31.20 mL of 99% formic acid mixed with 0.15 mL  
94 of cold water and 2.65 mL of 98% sulfuric acid and 5.43 mL of this mixture reacted with 6.89  
95 mL of 50% H<sub>2</sub>O<sub>2</sub> for 90 min in an ice bath). The resulting PFA stock solution contained  
96 approximately 19.5 ± 1.4% (233.9 ± 16.6 g/L) and 19.2 ± 1.2% (230.4 ± 13.8 mg/L) by weight  
97 of H<sub>2</sub>O<sub>2</sub> and PFA, respectively.

98 The quantification of high concentrations (>10 mg/L) of PFA and H<sub>2</sub>O<sub>2</sub> was performed using  
99 the iodometric method, as reported by Rocher & Azimi (Text S2, SI).<sup>6</sup> For PFA concentrations  
100 <10 mg/L, the measurement was performed with the DPD colorimetric method developed by  
101 Dominguez et al.<sup>22</sup> for PAA and adapted here for PFA (Text S2, Figure S1, SI).

## 102 2.3. Autodecomposition Kinetics of Peracids

103 The autodecomposition rates of PFA and PAA were determined either in DI water or in 10 mM  
104 phosphate buffer solution (PBS) at different pHs (from 2.3 to 11.0). After PFA titration by the  
105 iodometric method, the required volume of peracid was injected into 200 mL of PBS or DI  
106 water in a beaker to achieve a peracid initial concentration of 1.8 ± 0.3 mg/L for PFA and 0.4  
107 or 0.8 mg/L for PAA (respectively for pH 5.9 and 7.7). Samples were periodically taken to  
108 measure the residual peracid concentration by the DPD colorimetric method. All experiments  
109 were conducted at least in duplicate. Kinetic modeling was performed using COPASI.<sup>23</sup>

110 The autodecomposition of peracids followed first-order kinetics (eq 2).

$$\frac{d [\text{peracid}]}{dt} = - k_{\text{peracid}} \times [\text{peracid}] \quad (2)$$

111 Where  $k_{\text{peracid}}$  is the observed first-order rate constant for PFA or PAA and  $[\text{peracid}]$  is the  
112 concentration of PFA or PAA (mg/L).

113 The linearization of eq 2 (eq 3) showed a good fit with experimental values, confirming the  
114 first-order kinetics, and kinetic rate constants were derived from the slope of 3 and are expressed  
115 in  $\text{min}^{-1}$ .

$$\ln \left( \frac{[\text{peracid}]}{[\text{peracid}]_0} \right) = - k_{\text{peracid}} \times t \quad (3)$$

116 Where  $[\text{peracid}]_0$  is the initial concentration of PFA or PAA (mg/L).

#### 117 2.4. Reactivity of PFA with Inorganic and Organic Compounds

118 The reactivity of PFA was studied by examining its consumption by 45 compounds: 7 inorganic  
119 compounds (ammonia nitrogen, nitrite, bromide, iodide, chloride, iron(II), and hydrogen  
120 phosphate ions), 8 amino acids (glycine, methionine, cysteine, histidine, glutamine, tyrosine,  
121 tryptophan, and asparagine), 1 derived amino acid (taurine), 14 simple model organic  
122 compounds [morpholine, aniline, dimethylamine (DMA), trimethylamine (TMA), urea, furan,  
123 thiophene, resorcinol, phenol, hydroquinone, catechol, benzenethiol, 3-mercaptophenol and 4-  
124 aminophenol], and 15 pharmaceutical compounds (diclofenac, acetaminophen, lidocaine,  
125 naproxen, 17 $\alpha$ -ethinylestradiol, carbamazepine, sulfadiazine, sulfamethoxazole, ciprofloxacin,  
126 bisphenol A, tramadol, trimethoprim, ranitidine, furosemide and amoxicillin).

127 The 7 inorganic compounds were selected because they are typically present in WW, and some  
128 are known to interact with various oxidants, such as ozone,<sup>24</sup> chlorine,<sup>25,26</sup> and PAA.<sup>27</sup>  
129 Regarding organic compounds, it was important to first understand the degradation mechanisms  
130 of simple functional groups (using model organic compounds) before studying the reactivity of  
131 pharmaceuticals that typically contain multiple functional groups. The selection of  
132 pharmaceuticals was based on their frequent detection in Parisian WW,<sup>28</sup> while amino acids

133 were studied due to their common occurrence in WW as constituents of organic matter. Two  
134 sets of experiments were conducted: one in PBS (10 mM, pH 7.0) for all compounds and  
135 another in DI water (with the initial pH adjusted at 7.1 with NaOH before PFA addition) for  
136 iron(II) only. In all experiments, the solutions of the investigated compounds were prepared at  
137 8  $\mu\text{M}$ , and 16  $\mu\text{M}$  of PFA was added under stirring to initiate the reaction. After 10 min of  
138 reaction, aliquots of the solution were collected to measure the PFA consumption by each  
139 compound. All experiments were performed at least in triplicates and at  $20.0 \pm 1.0$  °C. The PFA  
140 consumption was normalized by dividing the residual concentrations of PFA in the solution  
141 containing the compound by the concentration in the solution of PFA alone (PFA control  
142 obtained by autodecomposition), resulting in the residual concentration ratio (RCR).

#### 143 2.5. Decomposition Kinetics of Model and Pharmaceutical Compounds

144 All decomposition kinetic rate constants were determined in 100 mL of PBS (10 mM, pH 7.0)  
145 containing 1  $\mu\text{M}$  of each molecule of interest. The working solution was placed under stirring  
146 in a thermostatic chamber at  $20.0 \pm 1.0$  °C (in an amber bottle and protected from light), and  
147 PFA was added to initiate the reaction ( $[\text{PFA}]_0 = 500$   $\mu\text{M}$ ). In order to be in pseudo-first-order  
148 and facilitate the calculation of kinetic rate constants, the initial concentration of the oxidant  
149 was 500 (PFA) or  $\sim 900$  times ( $\text{H}_2\text{O}_2$ ) that of the molecule. Under these conditions,  $\sim 30\%$  of the  
150 initial PFA concentration remained at the end of the reaction ( $\sim 150$   $\mu\text{M}$ ), which indicates that  
151 PFA was still in excess compared to the organic compound. At fixed time intervals, 1.5 mL of  
152 the sample was transferred to an amber vial containing 50  $\mu\text{L}$  of 0.1 M  $\text{Na}_2\text{S}_2\text{O}_3$   
153 ( $[\text{Na}_2\text{S}_2\text{O}_3]_0/[\text{PFA}]_0 = 7$ ) to stop the reaction before analysis (Section 2.7). Since  $\text{H}_2\text{O}_2$  (892  
154  $\mu\text{M}$ ,  $30.34 \pm 0.75$  mg/L) is always present in the PFA working solution (500  $\mu\text{M}$ , 31 mg/L),  
155 control experiments were conducted using pure  $\text{H}_2\text{O}_2$  at the same concentration as that present  
156 in the PFA solution in order to evaluate its contribution to decomposition kinetics. All kinetic



157 experiments were performed in triplicates with a maximum reaction time of 30 min. Sample  
158 vials were kept at 4 °C prior to analysis.

159 For all model and pharmaceutical compounds, the plots of  $\ln([\text{organic compound}]/[\text{organic}$   
160  $\text{compound}]_0)$  versus time showed good linearity, suggesting that the reaction was pseudo-first-  
161 order with respect to the organic compound, and the observed rate constant,  $k_{\text{obs}}$  ( $\text{min}^{-1}$ ), was  
162 derived from the slope. The decomposition of the model and pharmaceutical compounds by  
163 PFA can thus be described as second-order kinetics (eq 4), and the kinetic rate constants,  $k_{\text{app}}$   
164 ( $\text{M}^{-1} \text{s}^{-1}$ ), were calculated by dividing  $k_{\text{obs}}$  by the initial concentration of PFA.

$$\begin{aligned} & \frac{d [\text{organic compound}]}{dt} \\ &= - k_{\text{obs}} \times [\text{organic compound}] \\ &= - k_{\text{app}} \times [\text{PFA}] \times [\text{organic compound}] \end{aligned} \quad (4)$$

165 where  $k_{\text{obs}}$  ( $\text{min}^{-1}$ ) is the observed kinetic rate constant for the pseudo-first-order and  $k_{\text{app}}$   
166 ( $\text{M}^{-1} \text{s}^{-1}$ ) is the second-order rate constant for the organic compound; [PFA] and [organic  
167 compound] are the concentrations of PFA and the organic compound, respectively.

## 168 2.6. Reactions in Wastewater Effluent

169 Treated WW effluent was collected from the Seine Amont WWTP located in Valenton, France,  
170 as previously described.<sup>21</sup> Samples were collected directly before the discharge channel and  
171 were filtered upon arrival in the laboratory through a 0.7  $\mu\text{m}$  glass fiber filter (Whatman). The  
172 WW quality parameters were as follows (mean  $\pm$  standard deviation (SD) over three samples):  
173 pH  $7.9 \pm 0.1$ , total suspended solids  $5.5 \pm 2.8$  mg/L, UV254  $1.1 \pm 0.6$ , nitrite  $0.55 \pm 0.12$  mg/L  
174 as N, ammonium  $1.56 \pm 1.00$  mg/L as N, phosphate  $3.08 \pm 0.93$  mg/L as P, dissolved organic  
175 carbon  $8.06 \pm 0.73$  mg/L, and temperature  $22.9 \pm 0.6$  °C.

176 Batch oxidation experiments were conducted on the actual WW effluent without pH  
177 adjustment. The effluent was spiked with 7 pharmaceutical compounds at 1  $\mu\text{g/L}$  ( $\sim 4 \times 10^{-3}$   $\mu\text{M}$ )

178 each: ranitidine (RAN), lidocaine (LID), furosemide (FUR), diclofenac (DCF), acetaminophen  
179 (ACT), sulfamethoxazole (SMX), and carbamazepine (CBZ). The analysis of the non-spiked  
180 WW sample revealed the presence of these pharmaceuticals at various concentrations ( $C_0$ ,  
181 ranging from  $0.25 \mu\text{g/L}$  for SMX to  $1.25 \mu\text{g/L}$  for DCF, except RAN which was never detected,  
182 and FUR and ACT reached, respectively,  $\sim 3$  and  $15 \mu\text{g/L}$  in one sample). The 7 pharmaceuticals  
183 were spiked in WW in order to detect them after oxidation and to calculate their removals. PFA  
184 was added to the sample at 5 different concentrations (1, 2, 5, 10, and 100 mg/L equivalent to  
185 16, 32, 81, 161, and 1613  $\mu\text{M}$ ) under constant stirring.  $\text{Na}_2\text{S}_2\text{O}_3$  was added in excess after 1 h  
186 to stop the reaction before extraction and analysis (see Section 2.7). All experiments were  
187 conducted at least in duplicate.

## 188 2.7. Analytical Methods

189 Organic compounds used in kinetics experiments were quantified using high-performance  
190 liquid chromatography coupled to a diode array detection (HPLC-DAD, PD-M20A, Shimadzu).  
191 Analytical details (stationary and mobile phases elution gradient) are described in Text S3 (SI),  
192 and the operating wavelengths with maximum UV absorbance for all compounds are reported  
193 in Table S1 (SI).

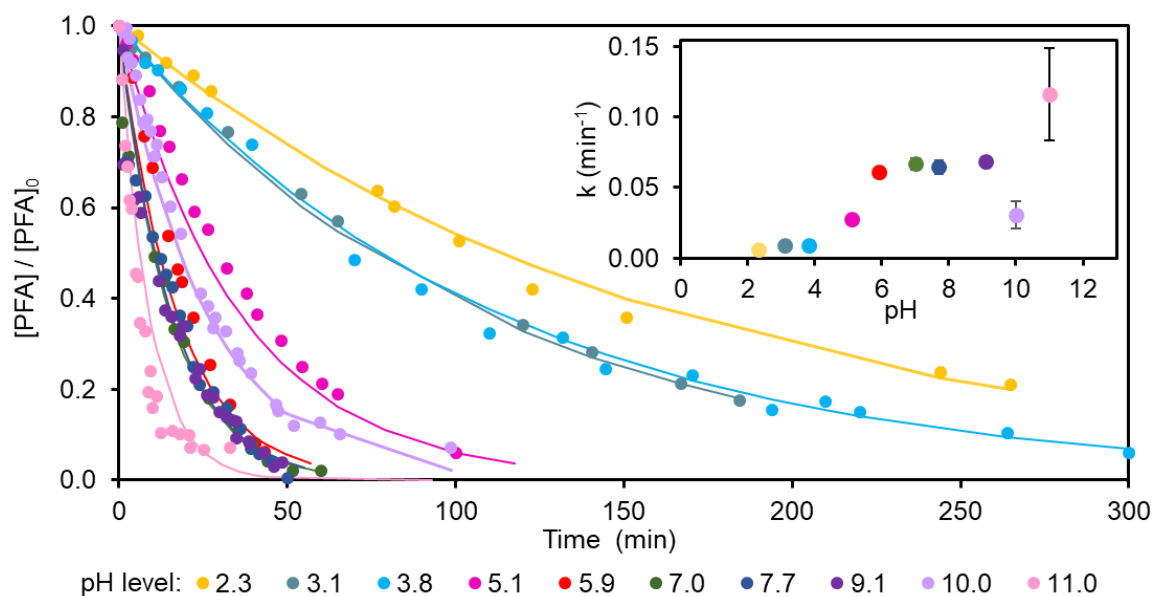
194 The 7 pharmaceutical compounds spiked in WW effluent samples were analyzed by ultrahigh-  
195 performance liquid chromatography (UPLC) coupled with tandem mass spectrometry (MS/MS)  
196 with triple quadrupole detection (Acquity-TQD, Waters) after extraction using an automated  
197 solid-phase extraction (SPE) system (Dionex Autotrace 280, Thermo Scientific) with multilayer  
198 SPE cartridges as described previously.<sup>21,29</sup> Analytical details (stationary and mobile phases,  
199 internal standards, elution gradient, and ionization mode) and the MS/MS acquisition  
200 parameters are provided in SI (Text S3, Table S2).

201 The transformation products (TPs) were characterized by high-resolution mass spectrometry  
202 (HRMS) using UPLC coupled with ion mobility time-of-flight mass spectrometry (Vion IMS-  
203 QToF, Waters) and equipped with an ESI source. The analysis was performed in both negative  
204 and positive ionization modes, and mass spectra were acquired in HDMS<sup>E</sup> (data independent  
205 analysis) mode to obtain low and high collision energy fragments. All information regarding  
206 the instrument parameters and the method was published previously.<sup>21</sup>

### 207 3. RESULTS AND DISCUSSION

#### 208 3.1. Autodecomposition Kinetics of Peracids

209 Since PFA solutions are unstable, the autodecomposition rates of PFA and PAA were  
210 determined at different pH levels (ranging from 2.3 to 11.0) in PBS (prior experiments showed  
211 no influence of phosphate ion, Text S4) to understand their behavior in the absence of other  
212 compounds. All autodecomposition experiments followed first-order kinetics for both PFA  
213 (Figure 1) and PAA (Figure S2).



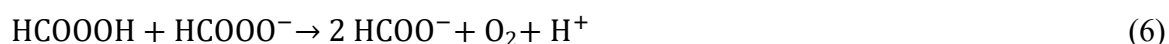
215 Figure 1. Autodecomposition of PFA in 10 mM phosphate buffer solution (PBS) at various  
216 initial pH levels, except for pH 3.8 representing the autodecomposition of PFA in DI water

217 without controlling pH (see Text S4).  $[PFA]_0 = 1.8 \pm 0.3$  mg/L ( $29 \mu\text{M}$ ). Errors bars on the rate  
218 constant values represent standard deviation from triplicate experiments.

219 The autodecomposition of PFA generally increased with increasing pH as reported for PAA,<sup>30,31</sup>  
220 showing similar decomposition rates between pH 5.9 and 9.1 and a decrease at pH 10.0 (Figure  
221 1). The autodecomposition of PFA was much slower at acidic pH ( $k_{PFA} = 6.1 \times 10^{-3}$ ,  $9.3 \times 10^{-3}$ ,  
222 and  $2.8 \times 10^{-2} \text{ min}^{-1}$  at pH 2.3, 3.1, and 5.1, respectively). Such a low degradation of PFA in  
223 acidic conditions and a higher degradation above pH 7.0 were reported in simulated combined  
224 sewer overflow waters.<sup>8</sup> This is in accordance with previous research showing that high acidity  
225 has a stabilizing effect on PFA.<sup>15</sup> In addition to its hydrolysis (reverse reaction in eq 1), PFA is  
226 generally considered to follow a decomposition reaction as described in eq 5.<sup>15,32,33</sup>



227 Kinetic modeling using eqs 1 and 5 could not explain the higher decomposition rates obtained  
228 near neutral pH and the restabilization at pH 10 because the kinetic constants proposed in the  
229 literature were obtained in acidic conditions (either with formic acid only or in the presence of  
230 sulfuric or phosphoric acid). The high decomposition rate observed in our study around the  $pK_a$   
231 value of PFA ( $7.1^{7,34}$ ) was consistent with a spontaneous decomposition of PFA by reaction  
232 between its acidic form (PFAH) and its basic form ( $\text{PFA}^-$ ) (eq 6), as reported for PAA in several  
233 studies.<sup>31,35,36</sup>



234 The decrease in PFA decomposition at pH 10 can thus be explained by a lower presence of  
235 PFAH, limiting the occurrence of this reaction. Base-catalyzed reactions with hydroxide ions  
236 ( $\text{OH}^-$ ) or the presence of carbonate ions (from the dissolution of carbon dioxide in the solution)

237 however probably played a role in the higher decomposition rate observed at pH 11. Kinetic  
238 modeling was attempted by introducing such reactions and the speciation of carbonate and  
239 phosphate ions (Figure S3D and E), but some discrepancies remained between the model and  
240 the experimental data (Table S3, Figure S4). Further research would be needed to fully elucidate  
241 the role of all present species and to provide a comprehensive kinetic model. In contrast to PFA,  
242 PAA was stable in both acidic and neutral pH conditions, and its lower autodecomposition was  
243 confirmed at pH 7.7 ( $k_{\text{PAA}} = 3.1 \times 10^{-3} \text{ min}^{-1}$  and  $k_{\text{PFA}} = 6.5 \times 10^{-2} \text{ min}^{-1}$ ) and at pH 5.9 ( $k_{\text{PAA}} =$   
244  $3.6 \times 10^{-3} \text{ min}^{-1}$  and  $k_{\text{PFA}} = 6.5 \times 10^{-2} \text{ min}^{-1}$ ) (Figure S2). This result agrees with previous  
245 findings that demonstrate the low decomposition of PAA in the pH range of 5.5 to 8.2.<sup>30</sup> In  
246 these experiments performed in DI water, the high stability of PAA compared to PFA can be  
247 attributed to its longer carbon chain, as aliphatic peracids tend to become more stable with  
248 longer chain lengths.<sup>37</sup>

### 249 3.2. Reactivity of PFA with Inorganic and Organic Compounds

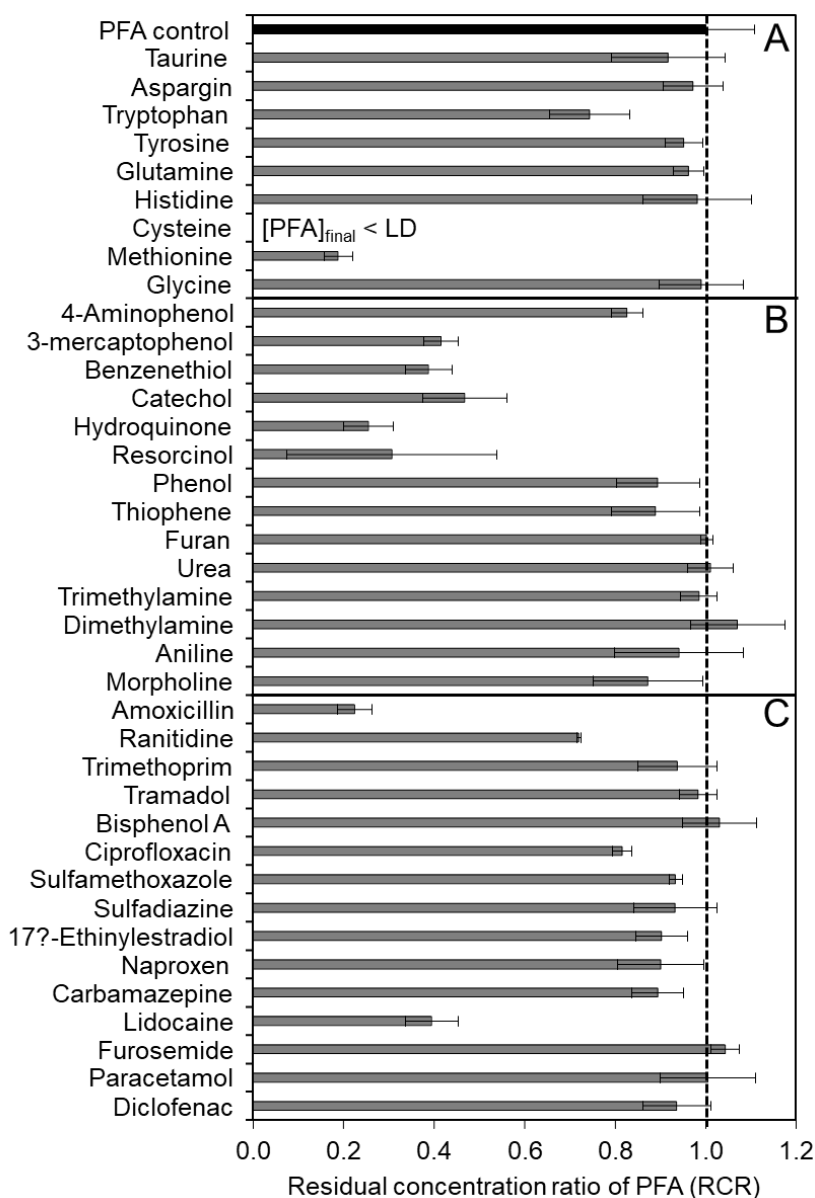
250 The reactivity of PFA with inorganic and organic compounds was first assessed by measuring  
251 the consumption of PFA by various compounds after 10 min of reaction to quickly identify the  
252 most reactive chemical structures. The PFA consumption results were expressed as residual  
253 concentration ratio (RCR, i.e., PFA residual normalized with the PFA autodecomposition).

254 Among the 7 inorganic ions studied (i.e., ammonia nitrogen, nitrite, bromide, iodide, chloride,  
255 iron(II) and hydrogen phosphate ions), only iodide ion consumed PFA in PBS (Figure S5). In  
256 DI water, reduced iron ( $\text{Fe}^{2+}$ ) exhibited a different reactivity, consuming around 20% of PFA  
257 (Figure S5). The difference in PFA consumption in PBS (pH 7.0) and DI water (pH 7.1) for  
258  $\text{Fe}^{2+}$  suggests that hydrogen phosphate ion can act as a chelating compound and decrease the  
259 consumption of PFA by  $\text{Fe}^{2+}$ . This effect has also been observed for PAA (DI water, pH 7.5),

260 where the presence of hydrogen phosphate ions decreased the impact of  $\text{Fe}^{2+}$  on PAA  
261 decomposition.<sup>27</sup>

262 Among the 9 amino acids, cysteine, methionine, and, to a lesser extent, tryptophan were the  
263 most reactive with PFA (Figure 2A). PFA was completely consumed by cysteine (RCR = 0),  
264 which is consistent with the high reactivity of cysteine with PAA<sup>38</sup> and the recent findings by  
265 Wang et al.,<sup>39</sup> showing the higher reactivity of cysteine and methionine with PFA. The  
266 reactivity of tryptophan with PFA is also in agreement with the reactivity of protein-like  
267 compounds (such as tryptophan and tyrosine) measured by fluorescence spectroscopy during  
268 the disinfection of WW.<sup>6</sup> In addition, the lack of PFA consumption by tyrosine, glutamine,  
269 histidine, and glycine, indicating their lower reactivity, is consistent with the results of Wang  
270 et al.,<sup>39</sup> who reported rate constants lower than  $0.1 \text{ M}^{-1} \text{ s}^{-1}$  for these amino acids at neutral pH  
271 (7.1).

272



273  
 274 Figure 2. Relative consumption of 16  $\mu\text{M}$  of PFA by 8  $\mu\text{M}$  amino acids (A), model organic  
 275 compounds (B), and pharmaceutical compounds (C) at pH 7.0,  $20.0 \pm 1.0$   $^{\circ}\text{C}$ , and 10 min of  
 276 reaction time. Results expressed as residual concentration ratio (RCR). The black bar  
 277 corresponds to the RCR of PFA self-decomposition (RCR = 1), and gray bars correspond to the  
 278 RCR of PFA in the presence of an organic compound. Values close to zero (as for cysteine)  
 279 indicate significant consumption of PFA.  $[\text{PFA}]_{\text{final}} < \text{LD}$  means that the residual concentration  
 280 of PFA is lower than the detection limit after 10 min of reaction.

282 PFA reacted with 9 of the 14 model organic compounds: resorcinol, hydroquinone,  
283 benzenethiol, 3-mercaptophenol, 4-aminophenol, thiophene, morpholine, aniline and phenol  
284 (Figure 2B). The reactivity of metalloles (derivatives of cyclopentadiene in which a carbon  
285 atom is replaced by a heteroatom) increased when they contained a sulfur heteroatom instead  
286 of an oxygen heteroatom (i.e., thiophene compared to furan). The strong reactivity of thiophene  
287 with PAA has been previously demonstrated during the oxidation of subbituminous carbons,  
288 resulting in the formation of sulfate ions or sulphone compounds.<sup>40</sup> PFA was slightly consumed  
289 by phenol and very slightly by aniline (considering the standard deviation of RCR results). The  
290 reactivity of substituted benzenic compounds largely increased with the addition of a second  
291 electron-donating group such as hydroxyl (–OH) (resorcinol, hydroquinone, and catechol  
292 compared to phenol, and 4-aminophenol compared to aniline). The presence of a thiol group  
293 (–SH) instead of hydroxyl (–OH) also dramatically increased the reactivity of the molecule  
294 (benzenethiol compared to phenol) but the addition of another –OH group to benzenethiol (3-  
295 mercaptophenol) did not increase its reactivity.

296 Out of the 15 pharmaceutical compounds investigated, 8 were found to react with PFA:  
297 amoxicillin, ranitidine, ciprofloxacin, sulfamethoxazole, sulfadiazine, 17 $\alpha$ -ethinylestradiol,  
298 carbamazepine, and lidocaine (Figure 2C). For naproxen and trimethoprim, no significant PFA  
299 consumption was observed given the variability of the results. PFA weakly reacted with some  
300 aromatic and amide compounds (e.g., 17 $\alpha$ -ethinylestradiol and carbamazepine) as well as  
301 compounds containing aromatic amine groups (e.g., sulfamethoxazole and sulfadiazine), in  
302 accordance with the results obtained with aniline. This reactivity of aromatic amine compounds  
303 was also demonstrated for PAA, with an oxygen attack occurring on the aromatic ring.<sup>41</sup> PFA  
304 was highly reactive with other organic compounds containing reduced-sulfur or nitrogen  
305 moieties (e.g., amoxicillin, ranitidine, and lidocaine). The high consumption of PFA by  
306 lidocaine is in accordance with a previous study and can be attributed to the reactivity of the



307 deprotonated tertiary amine group to form lidocaine N-oxide.<sup>21</sup> In contrast, the very low  
308 reactivity of tramadol, which also has a tertiary amine group, can be attributed to the absence  
309 of its deprotonated form at pH 7.0 ( $pK_a = 9.23$ ).<sup>21</sup> Carbamazepine, another compound with a  
310 tertiary amine moiety in a non-protonated form, also showed low consumption of PFA. This  
311 can be attributed to the higher stability of the nitrogen atom in the tertiary amine group due to  
312 steric hindrance and/or the electron-withdrawing effect of the aromatic rings and the carbonyl  
313 group.<sup>42</sup> The moderate consumption of PFA by ciprofloxacin can be explained by its secondary  
314 amine heteroatom group similar to morpholine that showed comparable consumption of PFA.  
315 Ciprofloxacin also has tertiary amine groups but similar to carbamazepine, they were probably  
316 not reactive due to their high stability and inability to be protonated (no  $pK_a$  on these nitrogen  
317 atoms) or attacked by oxygen. Compounds containing secondary amine groups (e.g.,  
318 diclofenac, acetaminophen, sulfadiazine, furosemide, or trimethoprim) did not consume or were  
319 very weakly reactive with PFA, which can be explained by similar stabilization effects.  
320 Dimethylamine and trimethylamine also did not consume any significant amount of PFA,  
321 indicating that N-oxide formation requires the presence of groups that destabilize the molecule  
322 (e.g., electron-donating groups). Given the low reactivity of PFA with phenol and  
323 primary/secondary amines, the high reactivity of amoxicillin should be attributed to other  
324 functional groups such as the thioether sulfur heteroatom. The reactivity of this thioether group  
325 of  $\beta$ -lactams has been demonstrated with PAA, generating sulfoxide products.<sup>43</sup> Taking into  
326 account all these results, the moderate consumption of PFA by ranitidine could be explained by  
327 the reactivity of both its thioether and deprotonated tertiary amine groups. Taurine, sulfadiazine  
328 and sulfamethoxazole, while sulfur-containing, have a fully oxidized sulfur atom (i.e., sulfonyl  
329 moiety,  $O=S=O$ ), which results in their very low PFA consumption, as previously reported for  
330 their reactivity with PAA.<sup>41</sup>

331 These results especially demonstrate the high reactivity of compounds containing reduced-  
332 sulfur moieties such as thiol and thioether groups (cysteine, methionine, benzenethiol, 3-  
333 mercaptophenol, amoxicillin, and ranitidine), as well as deprotonated tertiary amine groups  
334 destabilized by electron-donating groups. This reactivity follows similar trends as that of ozone  
335 since it has been demonstrated that tertiary amines have a higher reactivity with ozone than  
336 secondary amines due to the inductive effects of alkyl groups and also that the deprotonated  
337 form of amines is generally more reactive than the protonated form.<sup>42,44</sup>

### 338 3.3. Kinetics of Organic Compound Oxidation by PFA

339 Since PFA consumption could be biased by the presence of transformation products (TPs) with  
340 potential PFA reactivity, further experiments were carried out to study the oxidation kinetics of  
341 13 organic compounds (chosen among model and pharmaceutical compounds) by monitoring  
342 their degradation. A control experiment revealed that there was no significant difference in PFA  
343 consumption in the presence or absence of the organic compound (Figure S6). This supports  
344 the assumption of pseudo-first-order kinetics with respect to the organic compound and shows  
345 that in these conditions, PFA remained in excess and its degradation was mainly due to its  
346 autodecomposition (i.e., negligible consumption by organic compounds). Other control  
347 experiments also showed no contribution of background H<sub>2</sub>O<sub>2</sub> concentration to the degradation  
348 of organic compounds (Text S5).

#### 349 3.3.1. Kinetic Constants of Model Compounds

350 The kinetic constants of 6 model organic compounds, containing only one aromatic ring, were  
351 determined (Table 1). The compounds included 2 sulfur molecules containing thiol groups  
352 (benzenethiol and 3-mercaptophenol) and 4 phenolic molecules (phenol, resorcinol,  
353 hydroquinone, and catechol). The kinetic reactivities followed similar trends to PFA  
354 consumptions (Section 3.2), with sulfur molecules and benzenediols showing higher reactivity

355 compared to simple phenol. PFA completely oxidized benzenethiol and 3-mercaptophenol in  
356 less than 1 min (Table S4) so their rate constants ( $k_{\text{PFA}}$ ) were estimated to be greater than  $2 \times 10^2$   
357  $\text{M}^{-1} \text{s}^{-1}$ . The reactions of the 4 phenolic compounds followed second-order kinetics with respect  
358 to both the organic compound and PFA concentrations. Their apparent rate constants ( $k_{\text{app}}$ )  
359 ranged from  $0.04 \pm 0.01$  to  $3.04 \pm 0.06 \text{ M}^{-1} \text{s}^{-1}$  at pH 7.0, with phenol being the least reactive  
360 and catechol the most reactive molecule. The kinetic rate constants of the various types of  
361 benzenediols showed clear differences depending on the position of  $-\text{OH}$  substituents despite  
362 similar PFA consumption observed for them (Table 1 and Figure 2B). This confirms that adding  
363 a second  $-\text{OH}$  substituent to phenol plays a crucial role in the reactivity of phenolic compounds  
364 with PFA but also reveals that its relative position influences the oxidation rate. The ortho  
365 position of the  $-\text{OH}$  group in catechol enhanced its reactivity compared to hydroquinone (para  
366 position) and resorcinol (meta position). The enhanced reactivity of phenolic compounds  
367 containing multiple  $-\text{OH}$  substituents can be attributed to an increase in electron density from  
368 electron-donating groups, as previously observed for PAA.<sup>41</sup> The reported  $k_{\text{PAA}}$  values for  
369 phenol and catechol ( $0.08 \pm 0.04$  and  $33.00 \pm 0.40 \text{ M}^{-1} \text{s}^{-1}$  at pH 5, respectively<sup>41</sup>) were in the  
370 same range as  $k_{\text{PFA}}$  ( $0.04 \pm 0.01$  and  $3.04 \pm 0.06$  at pH 7.0, respectively) (Table 1).

### 371 3.3.2. Kinetic Constants of Pharmaceutical Compounds

372 The kinetics of 7 pharmaceutical compounds were studied (Table 1): ranitidine (RAN),  
373 lidocaine (LID), furosemide (FUR), diclofenac (DCF), acetaminophen (ACT),  
374 sulfamethoxazole (SMX), and carbamazepine (CBZ). Similar to PFA consumption, the highest  
375 reactivities were observed for compounds containing reduced-sulfur and deprotonated amine  
376 moieties. RAN (containing a thioether and a tertiary amine group) was fully degraded by PFA  
377 in less than 30 seconds, so its  $k_{\text{PFA}}$  was estimated to be greater than  $2 \times 10^3 \text{ M}^{-1} \text{s}^{-1}$ . LID and  
378 FUR (two secondary amines with no reduced-sulfur group) were moderately degraded with  
379  $k_{\text{PFA}}$  values of  $2.24 \pm 0.14$  and  $0.41 \pm 0.18 \text{ M}^{-1} \text{s}^{-1}$ , respectively. A similar kinetic rate constant

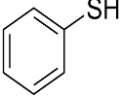
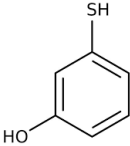
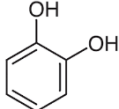
380 was obtained for LID in a previous study ( $k_{\text{PFA}} = 2.76 \pm 0.37 \text{ M}^{-1} \text{ s}^{-1}$  at pH 7.0).<sup>21</sup> Additional  
381 experiments performed with FUR confirmed the increase of its  $k_{\text{obs}}$  with increasing PFA  
382 concentrations, in accordance with second-order oxidation kinetics (Text S6, Figure S7). Three  
383 other pharmaceutical compounds (SMX, DCF, ACT) exhibited weaker reactivity with PFA  
384 (kinetic rate constants in the range from 0.11 to  $0.14 \pm 0.02 \text{ M}^{-1} \text{ s}^{-1}$ ), in the same range as those  
385 observed for simple phenolic molecules (Table 1). CBZ was the least reactive compound, with  
386 a rate constant of  $7.15 \pm 0.97 \times 10^{-3} \text{ M}^{-1} \cdot \text{s}^{-1}$ . Different trends between oxidation rate constants  
387 were observed compared to the PFA consumption of the same molecules (i.e., a lower PFA  
388 consumption of RAN than that of LID and a similar or even higher PFA consumption for CBZ  
389 than those of SMX, DCF, ACT, and FUR). As mentioned earlier, PFA consumption of some  
390 molecules could be increased by the formation of more reactive TPs, while some highly reactive  
391 molecules (e.g., RAN) could form less-reactive TPs resulting in decreased PFA consumption.

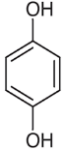
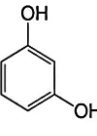
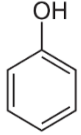
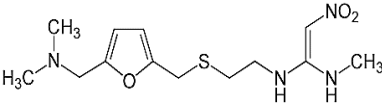
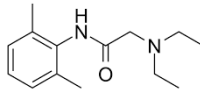
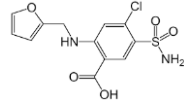
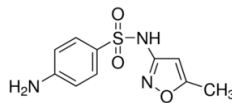
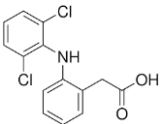
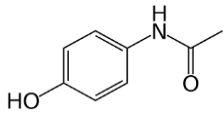
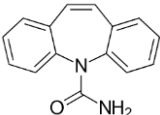
392 Similar to these results obtained with PFA, the high reactivity of reduced-sulfur compounds  
393 (e.g., cysteine and methionine) with PAA has been described, with  $k_{\text{PAA}}$  values ranging from  
394  $\sim 5$  to  $> 6 \times 10^2 \text{ M}^{-1} \text{ s}^{-1}$ .<sup>38</sup> The kinetic rate constants of cysteine and methionine have recently  
395 been evaluated for both PFA and PAA, with values reaching  $> 1 \times 10^5 \text{ M}^{-1} \text{ s}^{-1}$ .<sup>39</sup> This was  
396 attributed to the strong susceptibility of the reduced sulfur atom to electrophilic attack,  
397 corresponding to an electron transfer mechanism.<sup>38,39</sup> The  $k_{\text{PFA}}$  values of CBZ, SMX, DCF,  
398 ACT, FUR, and LID were in the same range as the  $k_{\text{PAA}}$  values reported for similar nitrogen-  
399 containing compounds (from  $2.5 \times 10^{-3}$  to  $1.6 \times 10^1 \text{ M}^{-1} \text{ s}^{-1}$ ).<sup>41</sup> The  $k_{\text{PFA}}$  of some investigated  
400 pharmaceutical compounds (SMX and DCF) were about 100 times higher than their reported  
401  $k_{\text{PAA}}$  values (Table 1).<sup>41</sup> Some other molecules exhibited lower reactivity with PFA than with  
402 PAA (i.e., 5 times lower  $k_{\text{PFA}}$  for CBZ, 10 times lower  $k_{\text{PFA}}$  for catechol, and a slightly lower  
403  $k_{\text{PFA}}$  for phenol). This suggests that PFA and PAA globally share similar reaction pathways for  
404 certain types of molecular groups, but the oxidation power of PFA can vary greatly depending

405 on the targeted molecule, being either lower or higher than that of PAA. This reactivity  
 406 difference could also be due to the pH values, as the  $k_{\text{PAA}}$  values were reported at pH 5.0,<sup>41</sup>  
 407 while the pH level in the present study was 7.0. Other differences in experimental conditions  
 408 (e.g., different buffer species, different ratios between reactive species, or the presence of  
 409 unknown reactive species formed during the degradation of peracids) could also play a role in  
 410 these different behaviors. Kinetics of LID and DCF decomposition at different pH showed a  
 411 much stronger reactivity at neutral or alkaline pH, suggesting a major role of the PFA  
 412 deprotonated form ( $\text{PFA}^-$ ) (Text S7, Figures S3, S8). An even more diverse set of molecular  
 413 structures should be investigated to fully understand the reactivity of PFA and potentially  
 414 predict the kinetic rates of organic molecules (e.g., with quantitative structure–activity  
 415 relationship models). Overall, PFA was found to be less oxidative than ozone toward the studied  
 416 pharmaceuticals, as indicated by the significantly higher kinetic rate constants reported in the  
 417 literature for ozone (from  $10^4$  to  $>10^6 \text{ M}^{-1} \text{ s}^{-1}$ ).<sup>45,46</sup>

418 Table 1. Second-Order Rate Constants ( $k_{\text{app}}$ ,  $\text{M}^{-1} \text{ s}^{-1}$ ) of Model Organic and Pharmaceutical  
 419 Compounds Oxidation by PFA. Experimental conditions:  $[\text{compound}]_0 = 1 \mu\text{M}$ ,  $[\text{PFA}]_0 =$   
 420  $500 \mu\text{M}$ .  $k_{\text{PAA}}$  from Kim & Huang<sup>41</sup> at pH 5.0 and 22.0 °C.

421

compounds	structure	$k_{\text{PFA}} (\text{M}^{-1} \text{ s}^{-1})$	$k_{\text{PAA}} (\text{M}^{-1} \text{ s}^{-1})$
benzenethiol		$> 2 \times 10^2$	
3-mercaptophenol		$> 2 \times 10^2$	
catechol		$3.04 \pm 0.06$	$3.33 \pm 0.40 \times 10^1$

hydroquinone		$0.80 \pm 0.21$	
resorcinol		$0.10 \pm 0.02$	
phenol		$0.04 \pm 0.01$	$8.00 \pm 0.40 \times 10^{-2}$
ranitidine		$> 2 \times 10^3$	
lidocaine		$2.24 \pm 0.14$	
furosemide		$0.41 \pm 0.18$	
sulfamethoxazole		$0.14 \pm 0.02$	$3.7 \pm 0.10 \times 10^{-3}$
diclofenac		$0.13 \pm 0.03$	$3.1 \pm 0.80 \times 10^{-3}$
acetaminophen		$0.11 \pm 0.02$	
carbamazepine		$7.15 \pm 0.97 \times 10^{-3}$	$3.4 \pm 0.40 \times 10^{-2}$

422

423 3.4. Influence of the PFA Dose in Environmental Water Matrices

424 The reactivity of the 7 pharmaceuticals for which oxidation kinetics are determined in Section

425 3.3 (RAN, LID, FUR, SMX, DCF, ACT, and CBZ) was investigated in real WW effluent to

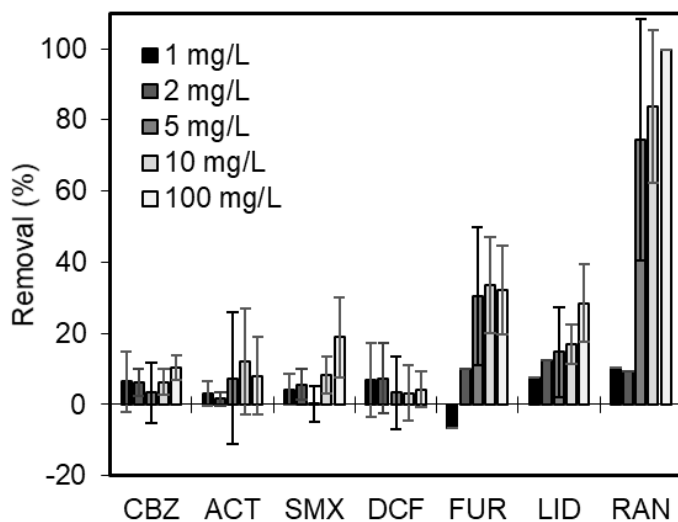
426 assess the effect of the WW matrix. The water quality parameters of the WW sample were  
427 described in Section 2.6.

428 The removal of the chosen micropollutants in real WW was low and very selective. RAN was  
429 the best-eliminated compound, and its removal increased from 10 to 99% when the PFA  
430 concentration varied between 1 and 100 mg/L (16 to 1613  $\mu\text{M}$ ) (Figure 3). CBZ, ACT, and  
431 DCF were recalcitrant to PFA oxidation, showing low removals (<10%) at all concentrations.  
432 SMX also exhibited low removals, but some increase was observed at 100 mg/L (1613  $\mu\text{M}$ ),  
433 reaching ~18%. FUR and LID were slightly removed at PFA concentrations <5 mg/L (81  $\mu\text{M}$ )  
434 and their removal significantly increased at higher concentrations. Contrary to RAN, their  
435 removal did not exceed 35% even at the highest concentrations. In addition, a slightly negative  
436 removal ( $-5\%$ ) was obtained for FUR at a 1 mg/L PFA concentration, which can be considered  
437 as not significant due to analytical uncertainties (e.g., discrepancies in the extraction of internal  
438 standards and matrix effects), especially at low concentrations of micropollutants.

439 Overall, even though most pharmaceuticals exhibited lower removals than expected after 1 h  
440 based on their oxidation rate constants in PBS, their reactivities in WW followed the same  
441 trends (Section 3.3), with RAN being the most reactive compound followed by LID and FUR.  
442 In PBS and at pH 7.0, 1  $\mu\text{M}$  of LID and FUR resulted in  $91 \pm 1$  and  $38 \pm 10\%$  removal,  
443 respectively, with 31 mg/L (500  $\mu\text{M}$ ) of PFA (Figure S9). At 100 mg/L (1613  $\mu\text{M}$ ) of PFA and  
444 at the pH of the WW effluent (7.9), it was expected that their removal rates would be even  
445 higher especially since LID has been found to be more reactive at pH 8.0 than at pH 7.0 ( $k_{\text{app}}$   
446 of  $2.24 \pm 0.14$  and  $7.54 \pm 0.90 \text{ M}^{-1} \text{ s}^{-1}$  at pH 7.0 and 8.0, respectively).<sup>21</sup> The decrease of  
447 organic micropollutants (OMP) removal in real WW can be related to the presence of total  
448 suspended solids (TSS), organic matter (OM), and other species that could consume PFA (e.g.,  
449 transition metals such as  $\text{Fe}^{2+}$ ,  $\text{Cu}^{2+}$ , and  $\text{Mn}^{2+}$ ) and thus compete with the OMP removal. More

450 systematic experiments (e.g., with synthetic OM) are needed to understand such competition  
451 effects during PFA oxidation.

452



453

454 Figure 3. Removal of pharmaceuticals in wastewater by PFA. Experimental conditions:  
455 [Pharmaceutical compound]<sub>0</sub> = C<sub>0</sub> + 1 μg/L (~4 × 10<sup>-3</sup> μM) spiked in WW, with C<sub>0</sub>, the initial  
456 concentration of the compound in the WW effluent, reaction time = 60 min, pH = 7.88 ± 0.10,  
457 20.0 °C, [PFA]<sub>0</sub> = 1, 2, 5, 10, and 100 mg/L (16, 32, 81, 161, 1613 μM). Error bars represent  
458 the standard deviation from triplicate samples.

459

### 460 3.5. Identification of Oxidation Byproducts

461 To better understand the oxidation mechanisms of organic compounds by PFA, TPs produced  
462 by the reaction between PFA and individual solutions of organic compounds in 10 mM PBS  
463 (pH 7.0) were characterized by HRMS. Among the model organic compounds (Sections 3.2  
464 and 3.3), only benzenethiol (BZT), 3-mercaptophenol (3MP), and catechol (CTL) were studied,  
465 as the other compounds or their TPs were not adequately detected. The exact masses of the  
466 parent compounds and their TPs, as well as their detection parameters and main fragments, are

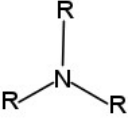
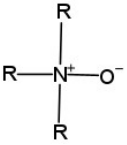
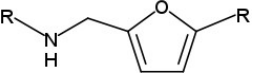
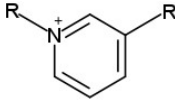
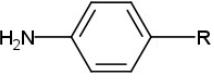
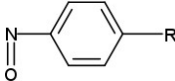
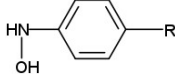
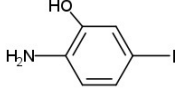


467 described in Tables S5 and S6, and the detailed identifications for each parent compound are  
468 described in Text S8 (SI).

469 For both model organic and pharmaceutical compounds, the addition of oxygen atoms on  
470 specific functional groups (such as thioether, thiol, and tertiary amine) was the major  
471 mechanism observed, with N-oxides, S-oxides, or hydroxylated compounds being the main  
472 observed types of TPs (Table 2). The oxidation of thiol compounds (BZT and 3MP) resulted in  
473 the addition of three oxygen atoms (i.e., sulfonic acid compounds), and the oxidation of the  
474 thioether group in RAN formed the S-oxide (1 additional oxygen atom) and sulfonyl (2 oxygen  
475 atoms) analogues. Compounds containing tertiary amine groups (RAN and LID) formed N-  
476 oxides (as previously reported for LID<sup>21</sup>), and SMX (aniline moiety) formed hydroxylated TPs.  
477 Similar mechanisms were reported for PAA oxidation<sup>38,41,43,47</sup> and ozonation,<sup>48,49</sup> suggesting  
478 similar sites of attack by these three oxidants. This is also in accordance with the higher  
479 reactivity of compounds containing reduced-sulfur or amine molecular groups (Sections 3.2  
480 and 3.3). The TPs of SMX confirmed that aniline is a reactive site, even if its reactivity is very  
481 weak (considering the low consumption of PFA by SMX, sulfadiazine and aniline itself). Other  
482 TPs with no addition of oxygen but a rearrangement of aromatic rings (pyridiniums) were also  
483 detected from FUR and RAN. The formation of pyridinium of FUR was previously reported  
484 during anodic oxidation or with electro-Fenton process.<sup>50,51</sup> The TPs identified in this study  
485 were chemically similar to their parent compounds, and almost no TPs of lower mass could be  
486 detected. This indicates a low transformation effect of PFA even for the most reactive  
487 compounds (i.e., sulfur-containing compounds such as RAN, BZT or 3MP), leading to their  
488 low mineralization. This should however be confirmed with other analytical techniques to target  
489 smaller, more polar or more volatile TPs (e.g., gas chromatography coupled to mass  
490 spectrometry).

491

492 Table 2. Reactive Sites of the Studied Organic Compounds with the Possible Pathways and  
 493 Produced Byproducts for PFA Oxidation, from the Most Reactive (1) to the Least Reactive (4)  
 494 Site (Based on Kinetic Constants Shown in Table 1).

reactive site of studied organic compounds	reactive site structure	reaction mechanism	possible oxidation byproducts (OBPs)
(1) reduced-sulfur moiety (thiol and thioether) (e.g., 3MP, BZT, RAN)	$R-SH$ $R-S-R$	O addition	$R-S(=O)-OH$ $R-S(=O)-R$ $R-S(=O)-R$
(2) tertiary amine (e.g., LID, RAN)		O addition	
(3) furan ring with secondary amine at the benzylic position (e.g., FUR, demethylated RAN)		ring rearrangement	
(4) aniline (e.g., SMX)		O addition, hydroxylation	  

495  
 496 N-oxides are known to be persistent and not biodegradable,<sup>44,52</sup> and some aromatic N-oxides  
 497 have been shown to induce genotoxicity or to be potential carcinogens.<sup>53,54</sup> The stability and  
 498 persistence of other main TPs produced from PFA (S-oxide, sulfonyl compounds) should thus

499 be evaluated to assess their potential impact in comparison to their parent molecules as well as  
500 their respective toxicity.

#### 501 4. ENVIRONMENTAL IMPLICATIONS

502 The increasing implementation of PFA disinfection units in WWTPs highlights the need to  
503 understand the effect of PFA on inorganic and organic compounds as well as its behavior under  
504 various conditions (e.g., pH, presence of OM). Autodecomposition experiments revealed that  
505 PFA was more stable in acidic conditions compared to neutral or alkaline conditions.  
506 Conversely, the oxidation of DCF and LID was more effective in alkaline conditions. The  
507 influence of the deprotonated form of PFA ( $\text{PFA}^-$ ) and its enhanced oxidation power while  
508 experiencing higher autodecomposition requires further investigation. Systematic PFA  
509 decomposition studies are still lacking to provide a comprehensive kinetic model that accurately  
510 reflects the behavior of PFA at various pH levels.

511 Major inorganic ions (such as ammonium, nitrite, bromide, chloride, and orthophosphate ions)  
512 did not consume PFA, indicating a low impact on the optimal dose of PFA to be used in  
513 WWTPs. PFA demonstrated a high selectivity towards specific organic moieties (e.g., reduced  
514 sulfur and tertiary amines), with apparent low transformation and mineralization of organic  
515 compounds, even for highly reactive ones (i.e., sulfur-containing compounds such as ranitidine,  
516 benzenethiol, or 3-mercaptophenol). This suggests a low concern for the formation of numerous  
517 and toxic TPs during PFA disinfection as compared to other oxidation processes. However, it  
518 is crucial to evaluate the stability, persistence, and potential toxicity of S-oxides, sulfonyl, or  
519 N-oxides compounds in the environment to assess their impact compared to their parent  
520 molecules. The high selectivity of PFA toward reduced sulfur is also consistent with recent  
521 findings showing its high reactivity with cysteine and methionine, responsible for its specific  
522 disinfection properties (i.e., bacterial inactivation through accumulation in cells and  
523 intracellular oxidation).<sup>39</sup>

524 Due to the presence of TSS, OM and/or transition metals, pharmaceutical compounds were less  
525 effectively eliminated in real WW compared to PBS. The impact of TSS has been observed on  
526 PFA disinfection,<sup>6</sup> but it would require further investigation regarding oxidation reactions as  
527 well as the competition between OM and micropollutants.

528 Overall, PFA does not appear to be an efficient oxidant for the advanced treatment of  
529 micropollutants. Therefore, future research could focus on its activation (e.g., through  
530 irradiation or metals) to enhance the removal of organic compounds while still utilizing its  
531 advantages in disinfection.

532

### 533 SUPPORTING INFORMATION

534 The Supporting Information is available free of charge e at

535 <https://pubs.acs.org/doi/10.1021/acsestwater.3c00279>.

536 Additional analytical details, effect of several parameters (phosphate ion, background H<sub>2</sub>O<sub>2</sub>  
537 concentration, PFA initial concentration, pH) on PFA autodecomposition and oxidation  
538 kinetics, additional kinetics results, species distribution diagrams of PFA and selected  
539 micropollutants or inorganic ions, HRMS detailed identifications and the corresponding  
540 reaction pathways, and HRMS spectra of micropollutants and their transformation products.

### 541 NOTES

542 The authors declare no competing financial interest.

### 543 ACKNOWLEDGMENTS

544 This work was conducted as part of the OPUR research program and received partial support  
545 from the WaterOmics program (ANR-17-CE34-0009-01). The authors also acknowledge the  
546 PRAMMICS Platform (OSU-EFLUVE UMS 3563) for their assistance with UPLC-IMS-

547 QTOF and HPLC-DAD analysis, Michael Rivard for synthesizing and providing pyridinium of  
548 furosemide, Maysar Bouslah, Melissia Ben-Iken, and Ilyess Taibi for their contributions to the  
549 experiments, and Lila Boudahmane for her assistance with laboratory experiments.

## 550 REFERENCES

- 551 (1) Campo, N.; De Flora, C.; Maffettone, R.; Manoli, K.; Sarathy, S.; Santoro, D.;  
552 Gonzalez-Olmos, R.; Auset, M. Inactivation Kinetics of Antibiotic Resistant Escherichia Coli  
553 in Secondary Wastewater Effluents by Peracetic and Performic Acids. *Water Research* **2020**,  
554 *169*, 115227. <https://doi.org/10.1016/j.watres.2019.115227>.
- 555 (2) Gehr, R.; Chen, D.; Moreau, M. Performic Acid (PFA): Tests on an Advanced Primary  
556 Effluent Show Promising Disinfection Performance. *Water Science and Technology* **2009**, *59*  
557 (1), 89–96. <https://doi.org/10.2166/wst.2009.761>.
- 558 (3) Karpova, T.; Pekonen, P.; Gramstad, R.; Öjstedt, U.; Laborda, S.; Heinonen-Tanski, H.;  
559 Chávez, A.; Jiménez, B. Performic Acid for Advanced Wastewater Disinfection. *Water Sci*  
560 *Technol* **2013**, *68* (9), 2090–2096. <https://doi.org/10.2166/wst.2013.468>.
- 561 (4) Kitis, M. Disinfection of Wastewater with Peracetic Acid: A Review. *Environment*  
562 *International* **2004**, *30* (1), 47–55. [https://doi.org/10.1016/S0160-4120\(03\)00147-8](https://doi.org/10.1016/S0160-4120(03)00147-8).
- 563 (5) Ragazzo, P.; Chiuccini, N.; Piccolo, V.; Spadolini, M.; Carrer, S.; Zanon, F.; Gehr, R.  
564 Wastewater Disinfection: Long-Term Laboratory and Full-Scale Studies on Performic Acid in  
565 Comparison with Peracetic Acid and Chlorine. *Water Research* **2020**, *184*, 116169.  
566 <https://doi.org/10.1016/j.watres.2020.116169>.
- 567 (6) *Effectiveness of Disinfecting Wastewater Treatment Plant Discharges: Case of*  
568 *Chemical Disinfection Using Performic Acid*; Rocher, V., Azimi, S., Eds.; IWA Publishing,  
569 2021. <https://doi.org/10.2166/9781789062106>.
- 570 (7) Luukkonen, T.; Heyninck, T.; Rämö, J.; Lassi, U. Comparison of Organic Peracids in  
571 Wastewater Treatment: Disinfection, Oxidation and Corrosion. *Water Research* **2015**, *85*, 275–  
572 285. <https://doi.org/10.1016/j.watres.2015.08.037>.
- 573 (8) Chhetri, R. K.; Thornberg, D.; Berner, J.; Öjstedt, U.; Sharma, A. K.; Andersen, H. R.;  
574 Andersen, H. R. Chemical Disinfection of Combined Sewer Overflow Waters Using Performic  
575 Acid or Peracetic Acids. *Science of The Total Environment* **2014**, *490*, 1065–1072.  
576 <https://doi.org/10.1016/j.scitotenv.2014.05.079>.
- 577 (9) Chhetri, R. K.; Flagstad, R.; Munch, E. S.; Hørning, C.; Berner, J.; Kolte-Olsen, A.;  
578 Thornberg, D.; Andersen, H. R. Full Scale Evaluation of Combined Sewer Overflows  
579 Disinfection Using Performic Acid in a Sea-Outfall Pipe. *Chemical Engineering Journal* **2015**,  
580 *270*, 133–139. <https://doi.org/10.1016/j.cej.2015.01.136>.
- 581 (10) Chhetri, R. K.; Baun, A.; Andersen, H. R. Algal Toxicity of the Alternative  
582 Disinfectants Performic Acid (PFA), Peracetic Acid (PAA), Chlorine Dioxide (ClO<sub>2</sub>) and  
583 Their by-Products Hydrogen Peroxide (H<sub>2</sub>O<sub>2</sub>) and Chlorite (ClO<sub>2</sub><sup>-</sup>). *International Journal*  
584 *of Hygiene and Environmental Health* **2017**, *220* (3), 570–574.  
585 <https://doi.org/10.1016/j.ijheh.2016.11.011>.

- 586 (11) Guzzella, L.; Monarca, S.; Zani, C.; Feretti, D.; Zerbini, I.; Buschini, A.; Poli, P.; Rossi,  
587 C.; Richardson, S. D. In Vitro Potential Genotoxic Effects of Surface Drinking Water Treated  
588 with Chlorine and Alternative Disinfectants. *Mutation Research/Genetic Toxicology and*  
589 *Environmental Mutagenesis* **2004**, *564* (2), 179–193.  
590 <https://doi.org/10.1016/j.mrgentox.2004.08.006>.
- 591 (12) Dell’Erba, A.; Falsanisi, D.; Liberti, L.; Notarnicola, M.; Santoro, D. Disinfection By-  
592 Products Formation during Wastewater Disinfection with Peracetic Acid. *Desalination* **2007**,  
593 *215* (1), 177–186. <https://doi.org/10.1016/j.desal.2006.08.021>.
- 594 (13) Ragazzo, P.; Chiucchini, N.; Piccolo, V.; Ostoich, M. A New Disinfection System for  
595 Wastewater Treatment: Performic Acid Full-Scale Trial Evaluations. *Water Science and*  
596 *Technology* **2013**, *67* (11), 2476–2487. <https://doi.org/10.2166/wst.2013.137>.
- 597 (14) Ragazzo, P.; Feretti, D.; Monarca, S.; Dominici, L.; Ceretti, E.; Viola, G.; Piccolo, V.;  
598 Chiucchini, N.; Villarini, M. Evaluation of Cytotoxicity, Genotoxicity, and Apoptosis of  
599 Wastewater before and after Disinfection with Performic Acid. *Water Research* **2017**, *116*, 44–  
600 52. <https://doi.org/10.1016/j.watres.2017.03.016>.
- 601 (15) Santacesaria, E.; Russo, V.; Tesser, R.; Turco, R.; Di Serio, M. Kinetics of Performic  
602 Acid Synthesis and Decomposition. *Ind. Eng. Chem. Res.* **2017**, *56* (45), 12940–12952.  
603 <https://doi.org/10.1021/acs.iecr.7b00593>.
- 604 (16) Luukkonen, T.; Pehkonen, S. O. Peracids in Water Treatment: A Critical Review.  
605 *Critical Reviews in Environmental Science and Technology* **2017**, *47* (1), 1–39.  
606 <https://doi.org/10.1080/10643389.2016.1272343>.
- 607 (17) Zhang, C.; Brown, P. J. B.; Hu, Z. Thermodynamic Properties of an Emerging Chemical  
608 Disinfectant, Peracetic Acid. *Science of The Total Environment* **2018**, *621*, 948–959.  
609 <https://doi.org/10.1016/j.scitotenv.2017.10.195>.
- 610 (18) Gagnon, C.; Lajeunesse, A.; Cejka, P.; Gagné, F.; Hausler, R. Degradation of Selected  
611 Acidic and Neutral Pharmaceutical Products in a Primary-Treated Wastewater by Disinfection  
612 Processes. *Ozone: Science & Engineering* **2008**, *30* (5), 387–392.  
613 <https://doi.org/10.1080/01919510802336731>.
- 614 (19) Cai, M.; Sun, P.; Zhang, L.; Huang, C.-H. UV/Peracetic Acid for Degradation of  
615 Pharmaceuticals and Reactive Species Evaluation. *Environ. Sci. Technol.* **2017**, *51* (24), 14217–  
616 14224. <https://doi.org/10.1021/acs.est.7b04694>.
- 617 (20) Ao, X.; Eloranta, J.; Huang, C.-H.; Santoro, D.; Sun, W.; Lu, Z.; Li, C. Peracetic Acid-  
618 Based Advanced Oxidation Processes for Decontamination and Disinfection of Water: A  
619 Review. *Water Research* **2021**, *188*, 116479. <https://doi.org/10.1016/j.watres.2020.116479>.
- 620 (21) Nihemaiti, M.; Huynh, N.; Mailler, R.; Mèche-Ananit, P.; Rocher, V.; Barhdadi, R.;  
621 Moilleron, R.; Le Roux, J. High-Resolution Mass Spectrometry Screening of Wastewater  
622 Effluent for Micropollutants and Their Transformation Products during Disinfection with  
623 Performic Acid. *ACS EST Water* **2022**, *2* (7), 1225–1233.  
624 <https://doi.org/10.1021/acsestwater.2c00075>.
- 625 (22) Domínguez-Henao, L.; Turolla, A.; Monticelli, D.; Antonelli, M. Assessment of a  
626 Colorimetric Method for the Measurement of Low Concentrations of Peracetic Acid and

- 627 Hydrogen Peroxide in Water. *Talanta* **2018**, *183*, 209–215.  
628 <https://doi.org/10.1016/j.talanta.2018.02.078>.
- 629 (23) Hoops, S.; Sahle, S.; Gauges, R.; Lee, C.; Pahle, J.; Simus, N.; Singhal, M.; Xu, L.;  
630 Mendes, P.; Kummer, U. COPASI—a COMplex PATHway SIMulator. *Bioinformatics* **2006**, *22*  
631 (24), 3067–3074. <https://doi.org/10.1093/bioinformatics/btl485>.
- 632 (24) Von Gunten, U. Ozonation of Drinking Water: Part II. Disinfection and by-Product  
633 Formation in Presence of Bromide, Iodide or Chlorine. *Water Research* **2003**, *37* (7), 1469–  
634 1487. [https://doi.org/10.1016/S0043-1354\(02\)00458-X](https://doi.org/10.1016/S0043-1354(02)00458-X).
- 635 (25) Le Roux, J.; Gallard, H.; Croué, J.-P. Chloramination of Nitrogenous Contaminants  
636 (Pharmaceuticals and Pesticides): NDMA and Halogenated DBPs Formation. *Water Research*  
637 **2011**, *45* (10), 3164–3174. <https://doi.org/10.1016/j.watres.2011.03.035>.
- 638 (26) Le Roux, J.; Gallard, H.; Croué, J.-P. Formation of NDMA and Halogenated DBPs by  
639 Chloramination of Tertiary Amines: The Influence of Bromide Ion. *Environ. Sci. Technol.*  
640 **2012**, *46* (3), 1581–1589. <https://doi.org/10.1021/es203785s>.
- 641 (27) Domínguez Henao, L.; Delli Compagni, R.; Turolla, A.; Antonelli, M. Influence of  
642 Inorganic and Organic Compounds on the Decay of Peracetic Acid in Wastewater Disinfection.  
643 *Chemical Engineering Journal* **2018**, *337*, 133–142. <https://doi.org/10.1016/j.cej.2017.12.074>.
- 644 (28) Guilloso, R.; Le Roux, J.; Mailler, R.; Vulliet, E.; Morlay, C.; Nauleau, F.; Gasperi,  
645 J.; Rocher, V. Organic Micropollutants in a Large Wastewater Treatment Plant: What Are the  
646 Benefits of an Advanced Treatment by Activated Carbon Adsorption in Comparison to  
647 Conventional Treatment? *Chemosphere* **2019**, *218*, 1050–1060.  
648 <https://doi.org/10.1016/j.chemosphere.2018.11.182>.
- 649 (29) Huynh, N.; Caupos, E.; Peirera, C.; Le Roux, J.; Bressy, A.; Moilleron, R. Evaluation  
650 of Sample Preparation Methods for Non-Target Screening of Organic Micropollutants in Urban  
651 Waters Using High-Resolution Mass Spectrometry. *Molecules* **2021**, *26*, 7064.  
652 <https://doi.org/10.3390/molecules26237064>.
- 653 (30) Yuan, Z.; Ni, Y.; Van Heiningen, A. R. P. Kinetics of Peracetic Acid Decomposition:  
654 Part I: Spontaneous Decomposition at Typical Pulp Bleaching Conditions. *Can. J. Chem. Eng.*  
655 **1997**, *75* (1), 37–41. <https://doi.org/10.1002/cjce.5450750108>.
- 656 (31) Yuan, Z.; Ni, Y.; Van Heiningen, A. R. P. Kinetics of the Peracetic Acid  
657 Decomposition: Part II: PH Effect and Alkaline Hydrolysis. *Can. J. Chem. Eng.* **1997**, *75* (1),  
658 42–47. <https://doi.org/10.1002/cjce.5450750109>.
- 659 (32) Sun, X.; Zhao, X.; Du, W.; Liu, D. Kinetics of Formic Acid-Autocatalyzed Preparation  
660 of Performic Acid in Aqueous Phase. *Chinese Journal of Chemical Engineering* **2011**, *19* (6),  
661 964–971. [https://doi.org/10.1016/S1004-9541\(11\)60078-5](https://doi.org/10.1016/S1004-9541(11)60078-5).
- 662 (33) Leveneur, S.; Thönes, M.; Hébert, J.-P.; Taouk, B.; Salmi, T. From Kinetic Study to  
663 Thermal Safety Assessment: Application to Peroxyformic Acid Synthesis. *Ind. Eng. Chem. Res.*  
664 **2012**, *51* (43), 13999–14007. <https://doi.org/10.1021/ie3017847>.
- 665 (34) Everett, A. J.; Minkoff, G. J. The Dissociation Constants of Some Alkyl and Acyl  
666 Hydroperoxides. *Trans. Faraday Soc.* **1953**, *49*, 410. <https://doi.org/10.1039/tf9534900410>.

- 667 (35) Koubek, E.; Haggett, M. L.; Battaglia, C. J.; Ibne-Rasa, K. M.; Pyun, H. Y.; Edwards,  
668 J. O. Kinetics and Mechanism of the Spontaneous Decompositions of Some Peroxoacids,  
669 Hydrogen Peroxide and *t*-Butyl Hydroperoxide. *J. Am. Chem. Soc.* **1963**, *85* (15), 2263–  
670 2268. <https://doi.org/10.1021/ja00898a016>.
- 671 (36) da Silva, W. P.; Carlos, T. D.; Cavallini, G. S.; Pereira, D. H. Peracetic Acid: Structural  
672 Elucidation for Applications in Wastewater Treatment. *Water Research* **2020**, *168*, 115143.  
673 <https://doi.org/10.1016/j.watres.2019.115143>.
- 674 (37) Swern, Daniel. Organic Peracids. *Chem. Rev.* **1949**, *45* (1), 1–68.  
675 <https://doi.org/10.1021/cr60140a001>.
- 676 (38) Du, P.; Liu, W.; Cao, H.; Zhao, H.; Huang, C.-H. Oxidation of Amino Acids by  
677 Peracetic Acid: Reaction Kinetics, Pathways and Theoretical Calculations. *Water Research X*  
678 **2018**, *1*, 100002. <https://doi.org/10.1016/j.wroa.2018.09.002>.
- 679 (39) Wang, J.; Chen, W.; Wang, T.; Reid, E.; Krall, C.; Kim, J.; Zhang, T.; Xie, X.; Huang,  
680 C.-H. Bacteria and Virus Inactivation: Relative Efficacy and Mechanisms of Peroxyacids and  
681 Chlor(Am)Ine. *Environ. Sci. Technol.* **2023**, acs.est.2c09824.  
682 <https://doi.org/10.1021/acs.est.2c09824>.
- 683 (40) Kato, T.; Uaciquete, D. L. E.; Onodera, G.; Okawa, H.; Sugawara, K.;  
684 Worasuwannarak, N. Changes in the Sulfur Forms of Subbituminous Coals during Oxidation  
685 with Hydrogen Peroxide and Peracetic Acid. *Fuel* **2022**, *330*, 125544.  
686 <https://doi.org/10.1016/j.fuel.2022.125544>.
- 687 (41) Kim, J.; Huang, C.-H. Reactivity of Peracetic Acid with Organic Compounds: A Critical  
688 Review. *ACS EST Water* **2021**, *1* (1), 15–33. <https://doi.org/10.1021/acsestwater.0c00029>.
- 689 (42) von Sonntag, C.; von Gunten, U. *Chemistry of Ozone in Water and Wastewater*  
690 *Treatment*; IWA Publishing, 2012; 312p, ISBN 978-1-78040-083-9.  
691 <https://doi.org/10.2166/9781780400839>
- 692 (43) Zhang, K.; Zhou, X.; Du, P.; Zhang, T.; Cai, M.; Sun, P.; Huang, C.-H. Oxidation of  $\beta$ -  
693 Lactam Antibiotics by Peracetic Acid: Reaction Kinetics, Product and Pathway Evaluation.  
694 *Water Research* **2017**, *123*, 153–161. <https://doi.org/10.1016/j.watres.2017.06.057>.
- 695 (44) Liu, X.; Yang, Z.; Zhu, W.; Yang, Y.; Li, H. Prediction of Pharmaceutical and Personal  
696 Care Products Elimination during Heterogeneous Catalytic Ozonation via Chemical Kinetic  
697 Model. *Journal of Environmental Management* **2022**, *319*, 115662.  
698 <https://doi.org/10.1016/j.jenvman.2022.115662>.
- 699 (45) Lee, Y.; Kovalova, L.; McArdell, C. S.; von Gunten, U. Prediction of Micropollutant  
700 Elimination during Ozonation of a Hospital Wastewater Effluent. *Water Research* **2014**, *64*,  
701 134–148. <https://doi.org/10.1016/j.watres.2014.06.027>.
- 702 (46) Altmann, J.; Ruhl, A. S.; Zietzschmann, F.; Jekel, M. Direct Comparison of Ozonation  
703 and Adsorption onto Powdered Activated Carbon for Micropollutant Removal in Advanced  
704 Wastewater Treatment. *Water Research* **2014**, *55*, 185–193.  
705 <https://doi.org/10.1016/j.watres.2014.02.025>.
- 706 (47) Emmons, W. D. The Oxidation of Amines with Peracetic Acid. *J. Am. Chem. Soc.* **1957**,  
707 *79* (20), 5528–5530. <https://doi.org/10.1021/ja01577a053>.



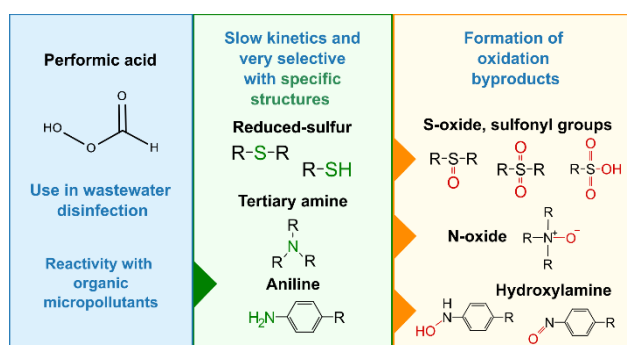
- 708 (48) Christophoridis, C.; Nika, M.-C.; Aalizadeh, R.; Thomaidis, N. S. Ozonation of  
 709 Ranitidine: Effect of Experimental Parameters and Identification of Transformation Products.  
 710 *Sci Total Environ* **2016**, *557–558*, 170–182. <https://doi.org/10.1016/j.scitotenv.2016.03.026>.
- 711 (49) Gulde, R.; Clerc, B.; Rutsch, M.; Helbing, J.; Salhi, E.; McArdell, C. S.; von Gunten,  
 712 U. Oxidation of 51 Micropollutants during Drinking Water Ozonation: Formation of  
 713 Transformation Products and Their Fate during Biological Post-Filtration. *Water Research*  
 714 **2021**, *207*, 117812. <https://doi.org/10.1016/j.watres.2021.117812>.
- 715 (50) Laurencé, C.; Rivard, M.; Lachaise, I.; Bensemoun, J.; Martens, T. Preparative Access  
 716 to Transformation Products (TPs) of Furosemide: A Versatile Application of Anodic Oxidation.  
 717 *Tetrahedron* **2011**, *67* (49), 9518–9521. <https://doi.org/10.1016/j.tet.2011.10.006>.
- 718 (51) Laurencé, C.; Rivard, M.; Martens, T.; Morin, C.; Buisson, D.; Bourcier, S.; Sablier,  
 719 M.; Oturan, M. A. Anticipating the Fate and Impact of Organic Environmental Contaminants:  
 720 A New Approach Applied to the Pharmaceutical Furosemide. *Chemosphere* **2014**, *113*, 193–  
 721 199. <https://doi.org/10.1016/j.chemosphere.2014.05.036>.
- 722 (52) Bourgin, M.; Beck, B.; Boehler, M.; Borowska, E.; Fleiner, J.; Salhi, E.; Teichler, R.;  
 723 von Gunten, U.; Siegrist, H.; McArdell, C. S. Evaluation of a Full-Scale Wastewater Treatment  
 724 Plant Upgraded with Ozonation and Biological Post-Treatments: Abatement of  
 725 Micropollutants, Formation of Transformation Products and Oxidation by-Products. *Water*  
 726 *Research* **2018**, *129*, 486–498. <https://doi.org/10.1016/j.watres.2017.10.036>.
- 727 (53) Zou, J.; Chen, Q.; Tang, S.; Jin, X.; Chen, K.; Zhang, T.; Xiao, X. Olaquinox-Induced  
 728 Genotoxicity and Oxidative DNA Damage in Human Hepatoma G2 (HepG2) Cells. *Mutation*  
 729 *Research/Genetic Toxicology and Environmental Mutagenesis* **2009**, *676* (1–2), 27–33.  
 730 <https://doi.org/10.1016/j.mrgentox.2009.03.001>.
- 731 (54) Chen, Y.; Zhang, H. Complexation Facilitated Reduction of Aromatic *N*-Oxides by  
 732 Aqueous Fe<sup>II</sup>-Tiron Complex: Reaction Kinetics and Mechanisms. *Environ. Sci. Technol.*  
 733 **2013**, *47* (19), 11023–11031. <https://doi.org/10.1021/es402655a>.

734

735

736 TOC Graphic

737



738

739